Bionatura
Latin American Journal of Biotechnology and Life Sciences

Bionatura Issue 3 Vol 8 No 1 2023

Article

Copper / Chitosan Nanocomposite Prepared by Chemical Method for Active Antimicrobial Activity

Ghufran K. Ibadi [1*], Ali A. Taha[2], and Selma M. H. Al-Jawad[3]
[1]Biomedical Engineering Department, University of Technology- Iraq.
[2]Biotechnology department, School of Applied Sciences, University of Technology- Iraq.
[3]Applied physics department, School of Applied Sciences, University of Technology- Iraq.
[*]Correspondence: 160006@uotechnology.edu.iq
Available from: http://dx.doi.org/10.21931/RB/CSS/2023.08.03.97

Abstract

Background: Chitosan is a promising polymeric that has received much attention recently. Chitosan nanoparticles have wide applications as a nanocarrier for different organic and inorganic substances. Materials and Methods: In the present study, copper (CuNPs), chitosan nanoparticles (CNPs) and Cu/CS nanocomposite (Cu/CNC) were prepared and characterized. All prepared nanoparticles were inspected by X-ray diffraction (XRD), Fourier transform infrared spectroscopy (FTIR), Field emission scanning electron microscope (FE-SEM), Energy Dispersive Spectroscopy (EDS), UV/VIS spectroscopy, and zeta potential. Finally, the antimicrobial activity of CuNPs, CNPs and Cu/CNC was tested by disc diffusion assay at different concentrations (0.5-2 mg/ml) against *Candida albicans*, *Klebsiella. pneumoniae* , *Pseudomonas aeruginosa* , *Proteus mirabilis* , *Cryptococcus sp.* , *Staphylococcus aureus*, *Escherichia coli*, and *Acinetobacter sp*. Results: The results showed an absorbance peak at 550 nm due to the presence of Cu/CNC. From the FTIR spectrum, a peak at 686.66 cm-1 refers to the copper successfully binding with chitosan. Furthermore, the particle size average of Cu/CNC was 36.34 - 48.27

Cu/CNC has the highest growth inhibition zone at a concentration of 2 mg/ml against *C.albicans*, *P.aeruginosa* and *S.aureus* with the diameters (9.75±0.35, 15±1.41, 15.5±0.70) mm, respectively. Conclusion: This study showed that Cu/CNC has higher antimicrobial activity than CNPs and CuNPs. It presented higher antibacterial activity against gram-negative bacteria than gram-positive bacteria.

Keywords: Copper nanoparticles, Chitosan nanoparticles, nanocomposite, XRD, FE_SEM Antimicrobial activity.

Introduction

Metal nanoparticles (MNPs) are tiny particles made of metal with the size (1-100) nm, and they have multiple properties according to the shape, size and composition that determine their catalytic, magnetic and other characteristics, such as silver, gold, copper, aluminum, iron, zinc and other metals [1]. Copper is a metal, a chemical element with a high melting point, high thermal and electrical conductivity, and large surface-to-volume ratio, and it is converted to copper nanoparticles (CuNPs) by chemical, physical, and biological methods. CuNPs were prepared by chemical method because it is a more suitable method, easily reproducible, economical, readily available, requires a low number of reagents, and a reaction temperature close to room temperature should be used [2]. CuNPs were used as antimicrobial, anticancer, agriculture, industrial, medical, and other applications because they have surface Plasmon resonance, which appears when it is transformed into CuNPs responsible for inhibiting the growth of bacteria and killing cancer cells [3,4]. CuNPs have antibacterial activity against gram-positive and gram-negative bacteria by accumulating on the surface of bacterial cells, leading to pores in the membrane, then entering the cell. The release of copper ions in the cell causes damage to DNA and cell death [5,6]. CuNPs are oxidized rapidly, and it is difficult to synthesize, so biopolymers such as chitosan and others are used to improve the stability of CuNPs [7].

Chitosan is a natural polymer obtained from the deacetylation of chitin. It contains N- acetyl -D-glucosamine and D-glucosamine subunits bounded by β (1,4) glycosidic bonds. It is converted to chitosan nanoparticles (CNPs) by Co-precipitation, ionic gelation, micro-emulsion, solvent evaporation and other methods. Due to the low toxicity, biodegradability and biocompatibility of CNPs, they can be used in several applications, such as wound healing, photothermal screening, antimicrobial, anticancer, and drug delivery [8].

In recent years, many types of literature have reported on synthesizing CNPs, CuNPs and Cu/CNC. Tyagi *et al.* have studied the preparation of chitosan nanoparticles by ionic gelation method, then used as antibacterial activity against *E. coli* and *S. aureus* [9]. Resmi *et al*. have studied the synthesis of CNPs from extracted shrimp shell waste and used their bactericidal activity against *E.coli*, *Pseudomonas aeruginosa*, *S. aureus* and *S. mutans* [10]. Fatma *et al*. have studied the synthesis of copper nanoparticles by the green method, which is used for antibacterial activity against *E.coli*, *Salmonella typhimurium*, and *Acetobacter aceti* [11]. Yaqub *et al*. have studied the preparation of CuNPs by chemical method and then tested via antimicrobial activity against *E.coli* and *Pseudomonas aeruginosa* [12].

Furthermore, Covarrubias *et al*. have studied the synthesis of copper/chitosan nanocomposite for antibacterial activity against *Streptococcus mutans* [7]. Arjunan *et al*. studied the preparation of Cu/CNC and then examined its antimicrobial activity against *Staphylococcus aureus*, *Streptococcus pneumoniae, P.aeruginosa*, *Proteus vulgaris* and *Candida albicans* [4]. When shown this report, notices not

finding CNPs, CuNPs and Cu/CNC in one report and not studying six strains of bacteria and two strains of fungi. So, in our research, we studied the synthesis of CNPs, CuNPs, and Cu/CNC by chemical method, and then we identified structural, morphological, and optical characterization. Following, CNPs, CuNPs and Cu/CNC were examined for antimicrobial activity against six strains of bacteria (*S. aureus*, *E. coli*, *P. aeruginosa*, *Proteus mirabilis*, *K. pneumonia, and Acinetobacter sp.*) and two strains of fungi (*C. albicans, Cryptococcus sp.*) at duplicate with concentrations (0.5, 1, 1.5 and 2) mg/ml by disc diffusion assay.

Materials and Methods

Synthesis of chitosan nanoparticles (CNPs): Chitosan (0.5 g) dissolved in 2% acetic acid under magnetic stirring for 30 min. The gelation solution of dissolved chitosan was sonicated for 10 min at 37 °C. Then 50 ml of methanol was added by dropper instead of double deionized water and 0.05% of Tween 80 with magnetic stirring at room temperature for 1 hour to form a homogenous solution. After obtaining the homogenous solution, 0.05% of sodium tripolyphosphate (STTP) was added gradually to the chitosan solution under magnetic stirring for 2 hours, and after each 30 min, sonication to disperse nanoparticles. Finally, it was centrifuged and washed 1-3 until pH reached (7.0) to obtain pure CNPs.

Synthesis of copper nanoparticles (CuNPs): CuNPs were synthesized by the chemical reduction method. Two grams of starch were dissolved in 100 ml DW under magnetic stirring at 100 °C for 30 min. Then cooled and mixed with 2 g of copper sulfate, 21 g of potassium sodium tartrate and 6 g of NaOH and stirred for 10 min. After that, 10 ml of formaldehyde was added to the mixture with magnetic stirring for 45-60 min until change the color of the reaction from blue to brownish red. Then, it was centrifuged, washed 1-3 times until pH reached 7.0 and dried.

Synthesis of copper/chitosan nanocomposite (Cu/CNC): Cu/CNC were prepared by dissolving 0.5 g of chitosan in 2% acetic acid and mixed with 0.05 g of CuNPs under magnetic stirring at 80 °C for 1 hour. The solution was centrifuged and washed 1-3 times until pH reached 7.0.

Characterization of nanoparticles and nanocomposite:

Nanoparticles and nanocomposite were measured using UV/VIS-spectrophotometry (Shimadzu, Japan) to confirm nanoparticle formation. FTIR analysis (Shimadzu, Japan) to identify functional groups of NPs in the range 400-4000 cm^{-1}. XRD (Philips, Holanda) to determine the structure of particles and zeta potential (Zetasizer Nano, Malvern, UK) to determine the stability and surface charge of nanoparticles. FE-SEM (TESCAN, Czech) to identify the size and morphology of nanoparticles and EDS analysis to determine the chemical elements of nanoparticles.

Antimicrobial activity of nanoparticles and nanocomposite:

The antimicrobial activity of nanoparticles and nanocomposite is performed by disc diffusion. Antibacterial activity of all nanoforms was determined against *S. aureus, E.coli, P. aeruginosa, Proteus mirabilis, K. pneumoniae, Acinetobacter sp.*, on Muller-Hinton agar plates (pH 7), while antifungal activity against *Candida albicans* and *Cryptococcus sp.* were examined on Sabouraud agar (pH 5.6). Moreover, bacterial inoculation size includes 1.5 $*10^8$ CFU/ml (McFarland standard tube No. 0.5), collected from 24-hour growth cultures, and the optical density at 600 nm (OD_{600}) measured in a spectrophotometer. On the other hand, fungal inoculation size adjusted to $10^6 – 5*10^6$ spores/ ml, obtained from 2-3 days old fungal growth cultures, by microscopic enumeration with cell–counting hematocytometer (Neubauer chamber, Merk, S.A., Madrid, Spain). The optical density at 530 nm (OD_{530}) of the spores suspension was measured in a spectrophotometer. After media inoculation, a sterilized filter paper disc (6 mm diameter) was loaded with 20 µl of different NPs or Cu/ CNC in duplicate with concentrations (0.5, 1, 1.5, 2 mg /ml) and placed on the agar surface. The bacterial inoculated plates were incubated at 37 °C for 24 hours, while incubation temperatures of 25 and 30 °C for 24 and 72 hours for both fungal strains, respectively. The diameter of the growth inhibition zone was measured in mm.

Results

Characterization analysis of nanoparticles and nanocomposite

X-ray diffraction analysis

The crystal structure of nanoparticles and nanocomposite was measured by XRD analysis. Figure 1., shows the XRD of CNPs, CuNPs and Cu/CNC.

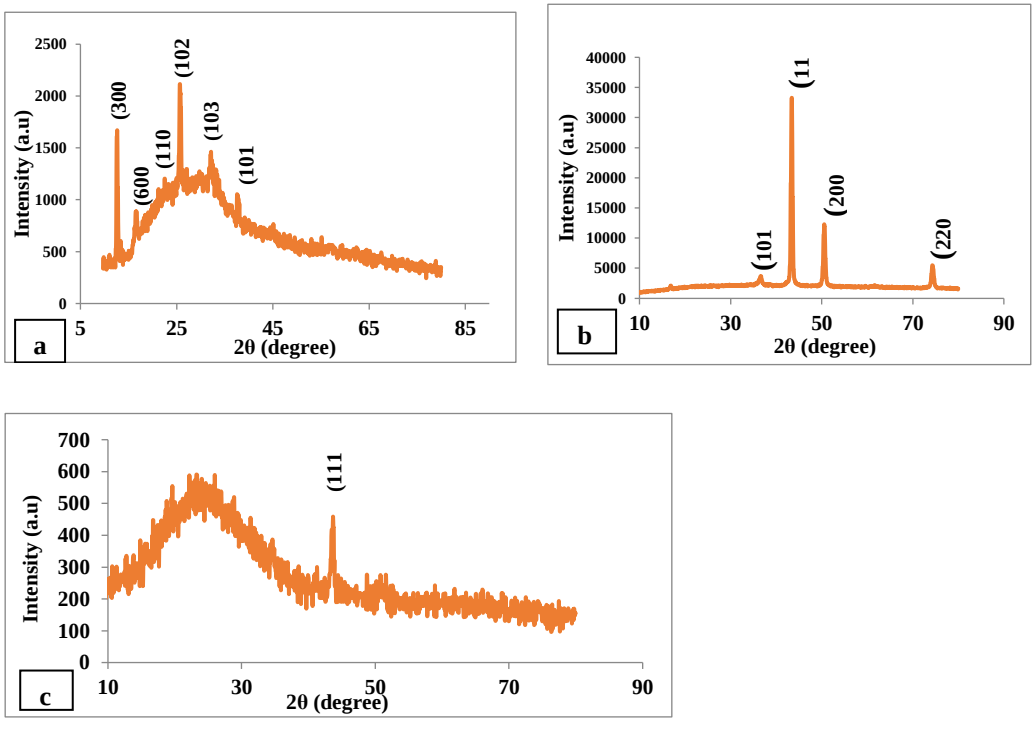

Figure 1. XRD patterns of (a) CNPs, (b) CuNPs and (c)Cu/CNC.

Fourier Transform Infrared Spectroscopy Analysis

FTIR spectrum is used to determine functional groups of nanoparticles and nanocomposites. The FTIR of CNPs, CuNPs, and Cu/CNC is seen in Figure 2.

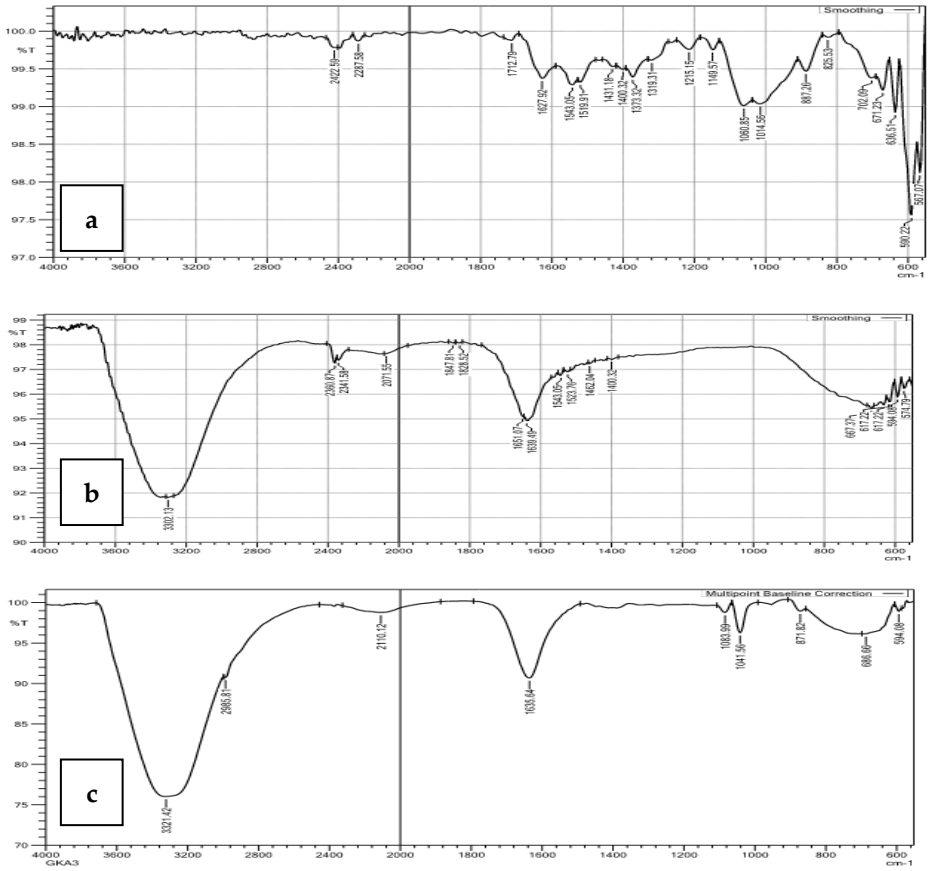

Figure 2. FTIR spectra of (a) CNPs, (b) CuNPs and (c) Cu/CNC.

FE-SEM and EDS analysis

FE-SEM is used to determine the size and morphology of CNPs, CuNPs and Cu/CNC, as shown in Figure 3. On the other hand, the chemical composition of nanoparticles and nanocomposite were identified by EDS analysis, as shown in Figure 4.

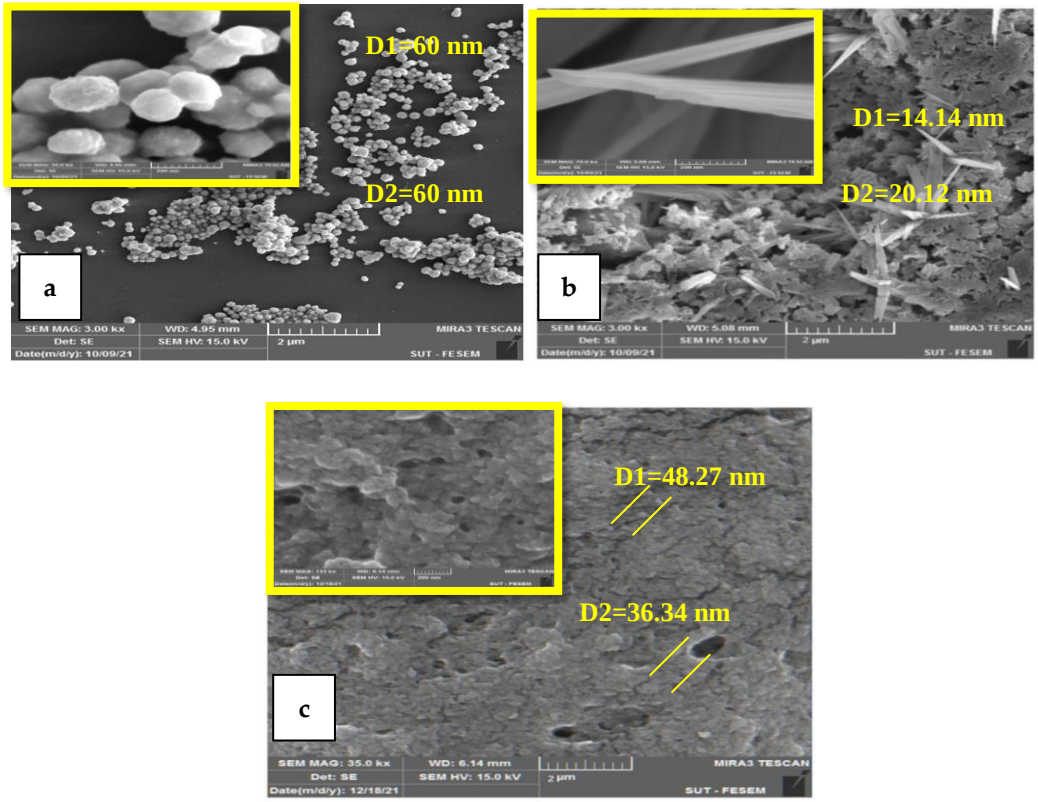

Figure 3. FE-SEM images of (a) CNPs, (b) CuNPs, (c) Cu/CNC.

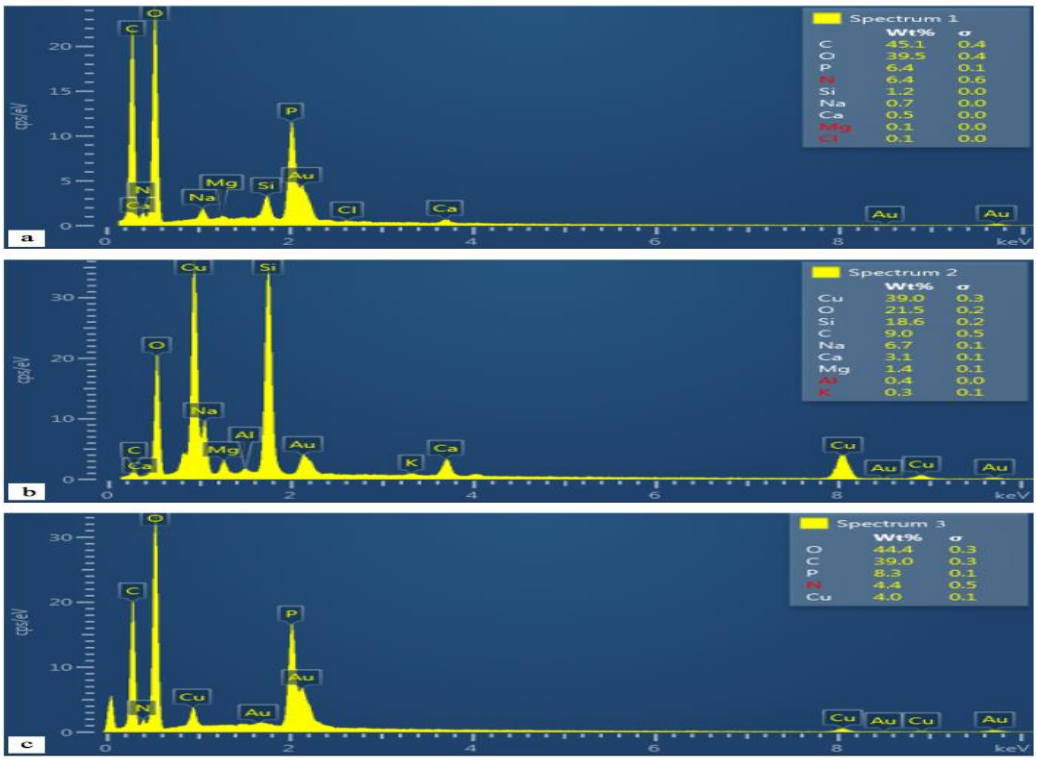

Figure 4. EDS patterns of (a) CNPs, (b) CuNPs, (c) Cu/CNC.

UV /VIS spectroscopy analysis

The peak absorption of chitosan nanoparticles was present at 225 nm, and no other optical absorption appeared. This indicates that the CNPs are pure, and these results agreed with those in [13], as shown in Figure 5a. On the other hand, the absorption peak of CuNPs obtained at 576 nm Figure 5b proved the oxidization form, and it has a strong surface Plasmon resonance (SPR) as determined by [14]. SPR is produced from the interaction of nanoparticles with the incident light. The free electrons in the copper metal's conduction band oscillate collectively due to this interaction. SPR considers the spectroscopic property of noble metal nanoparticles that lead to the presence of an absorption band in the visible range[15]. Furthermore, the absorption peak of Cu/CNC at 540 nm Figure 5c, refers to the chitosan interaction with copper, as mentioned by [4].

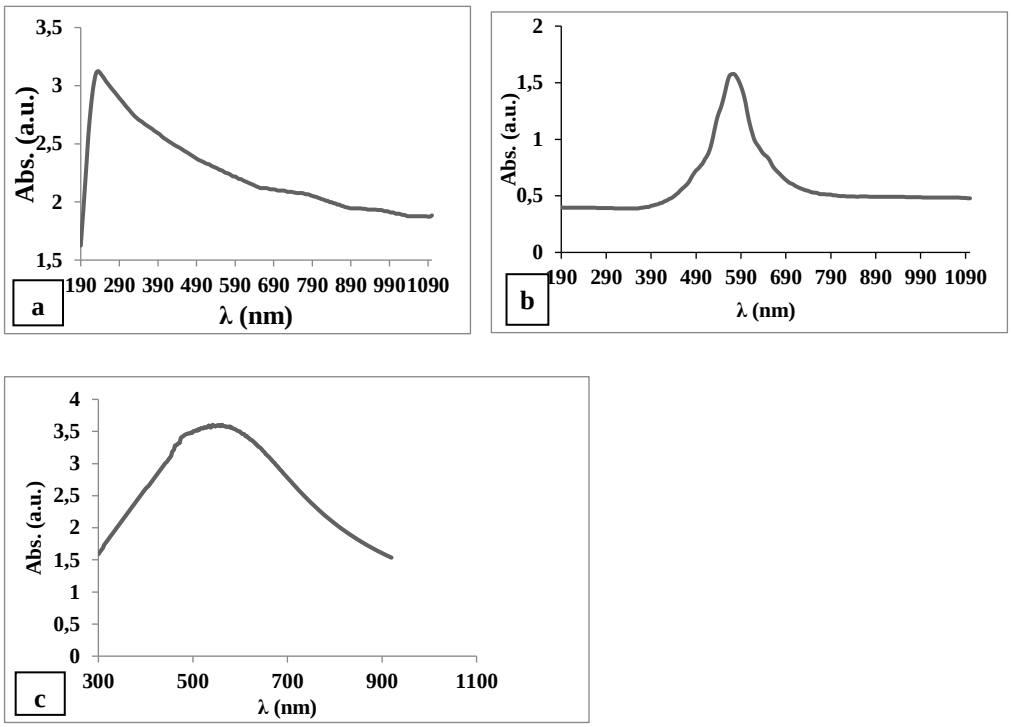

Figure 5. UV/VIS spectra of (a) CNPs, (b) CuNPs and (c) Cu/CNC.

Zeta Potential Analysis

The stability and uniformity of the nanomaterials were followed up by examining the zeta potential. The zeta potential values of CNPs, CuNPs and Cu/CNC were 10.7, -44.4 and 15.8 mV, respectively, as shown in Figure 6.

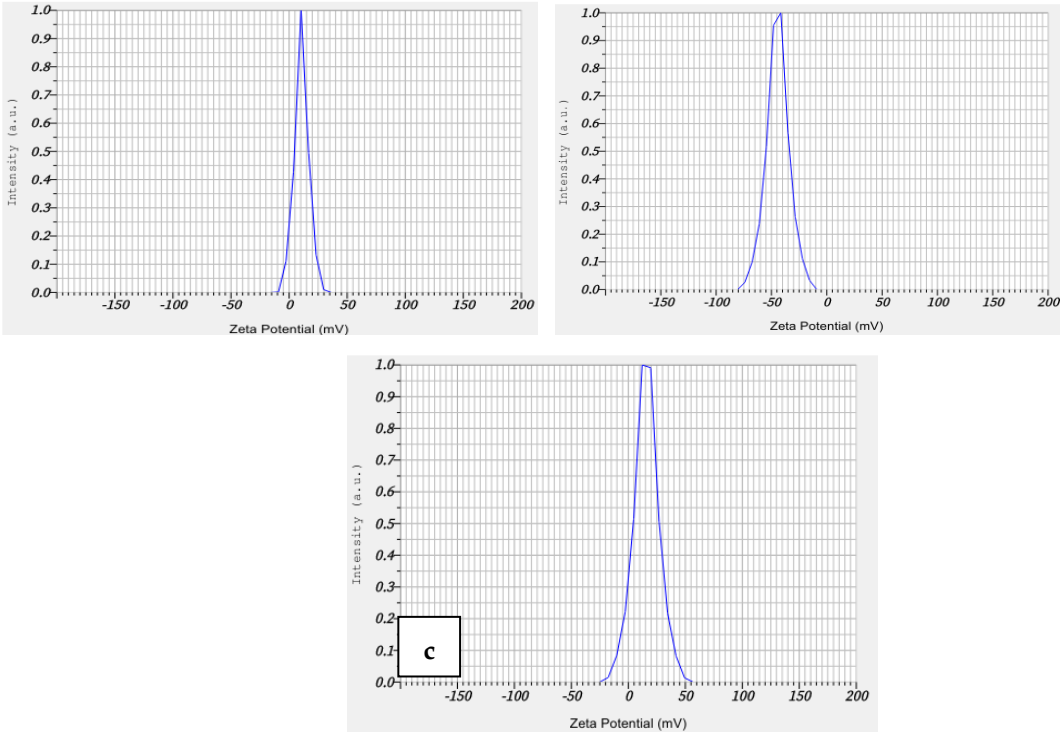

Figure 6. Zeta potential of (a) CNPs, (b) CuNPs, (c) Cu/CNC.

Antimicrobial activity of nanoparticles and nanocomposite

CNPs, CuNPs and Cu /CNC showed inhibitory activity against six bacterial strains (*S. aureus*, *E. coli*, *P. aeruginosa*, *Proteus mirabilis*, *K. pneumoniae*, *Acinetobacter sp.*) and two fungal strains (*C. albicans*, *Cryptococcus sp.*). CNPs and CuNPs appeared in high growth inhibition zone at different concentrations against *C. albicans* followed by *P. aeruginosa*, *K. pneumoniae*, *Proteus mirabilis*, *Cryptococcus sp.*, *S. aureus*, *Acinetobacter sp.* and *E. coli*, as see in the Tables 1 and 2. The growth inhibition zone caused by Cu/CNC in the presence of bacterial and fungal strains is shown in Tables (1 and 2). The higher growth inhibition zones at concentrations 2 mg/ml of 9.75±0.35, 15±1.41 and 15.5±0.70 mm appeared against *S. aureus*, *P. aeruginosa* and *C. albicans*, respectively. However, it decreased at concentration 0.5 mg/ml to 7±0, 7.5±0.70 and 8.25±0.35 mm, which refers to when the increased concentration of nanoparticles and nanocomposite leads to increased toxicity to bacterial and fungal strains causing growth inhibition and death of cells, as shown in Figures (7-9 C).

Samples	**Con. (mg/ml)**	**Growth inhibition zone (mm) of**					
		S. aureus	***E. coli***	***P.aeruginosa***	***Proteus mirabilis***	***K.pneumoniae***	***Acinetobacter sp.***

		Mean	S.D	Mean	S.D	Mean	S.D	Mean	S.D	Mean	S.D	Mean	S.D
CNPs	**0.5**	7	0	6.75	0.35	7.25	0.35	7.5	1.41	7.75	0.35	6.1	0.14
	1	7.5	0	7	0	8.5	2.12	7.1	0.14	8.25	0.35	6.5	0
	1.5	8.1	0.14	7.35	0.07	9	1.41	8.1	0.14	9.25	0.35	7	0
	2	8.5	0.70	7.75	0.07	11	1.41	10.75	0.35	11	1.41	8	0
CuNPs	**0.5**	7.25	0.35	6.5	0	7.5	0.70	6.25	0.35	6.75	0.35	6.1	0.14
	1	7.5	0.70	7	0	9	1.41	6.9	0.56	7.5	0.70	6.3	0.14
	1.5	7.5	0.70	7.75	0.35	10.1	0.14	7.4	0.14	8.8	0.56	6.8	0.28
	2	8.5	0.70	8.25	0.35	12.25	0.35	8.6	0.56	10.6	0.84	7.1	0.14
Cu/CNC	**0.5**	7	0	6.35	0.21	7.5	0.70	7.75	0.35	7.75	0.35	6.15	0.21
	1	7.5	0.70	7.3	0.14	10.5	0.70	8.25	0.35	10.5	0.70	6.4	0.42
	1.5	8	1.41	7.9	0.14	12.5	0.70	8.75	0.35	12	2.82	6.75	0.35
	2	9.75	0.35	8.5	0.14	15	1.41	10.25	1.06	14.5	0.70	7.95	1.20

Table 1. The diameters of gram-positive and negative bacteria growth inhibition zone (mm), mean, and standard deviation in the presence of CNPs, CuNPs and Cu/CNC.

Samples	**Concentration (mg/ml)**	**Growth inhibition zone (mm) of**			
		C. albicans		***Cryptococcus sp.***	
		Mean	**S.D**	**Mean**	**S.D**
CNPs	**0.5**	8.75	1.06	6.3	0.42
	1	10.25	0.35	7.45	0.07
	1.5	10.5	0.70	8.3	0.14
	2	12	1.41	9.85	0.91
CuNPs	**0.5**	8	1.41	6.75	0.35
	1	9.5	1.41	7.8	0.28
	1.5	11.5	0.70	8.2	0.28
	2	12.5	0.70	9.15	0.07
Cu/CNC	**0.5**	8.25	0.35	7.15	0.21
	1	10.75	3.18	8.35	0.21
	1.5	12	1.41	9.15	0.21
	2	15.5	0.70	10.5	0.14

Table 2. The diameters of fungal strains' growth inhibition zone (mm), mean, and standard deviation in the presence of CNPs, CuNPs and Cu/CNC.

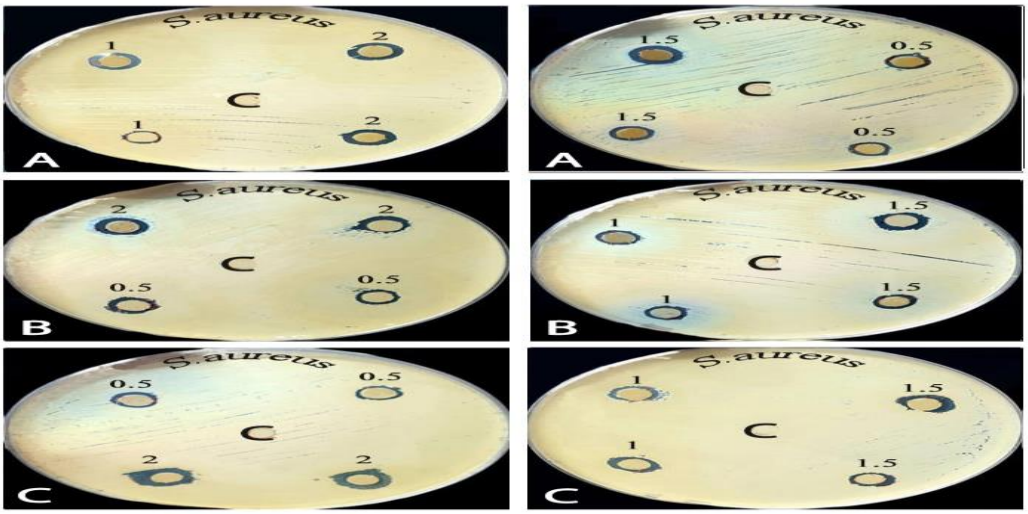

Figure 7. The effect of (A) CNPs, (B) CuNPs and (C) Cu/CNC on S. aureus.

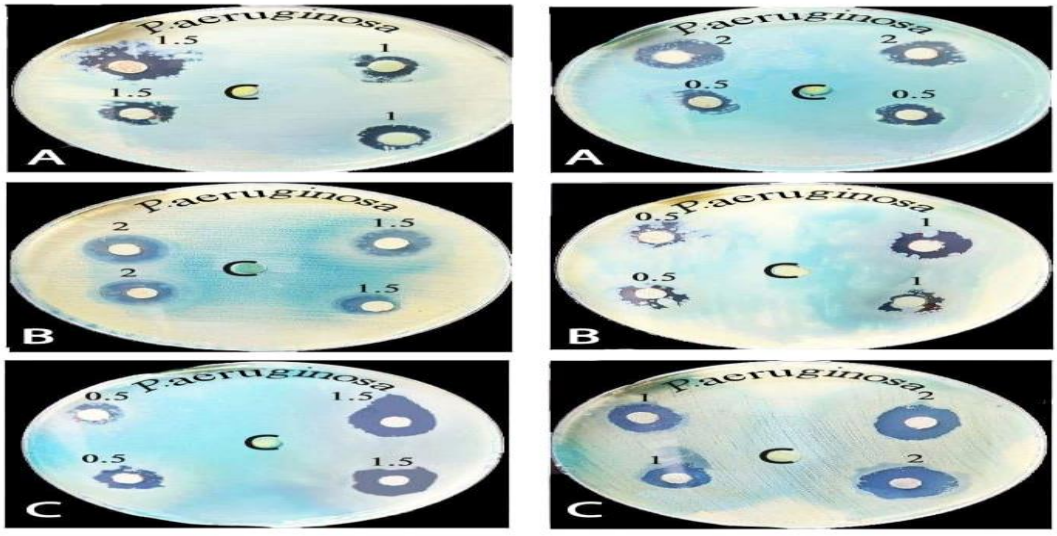

Figure 8. The effect of (A) CNPs, (B) CuNPs and (C) Cu/CNC on P. aeruginosa.

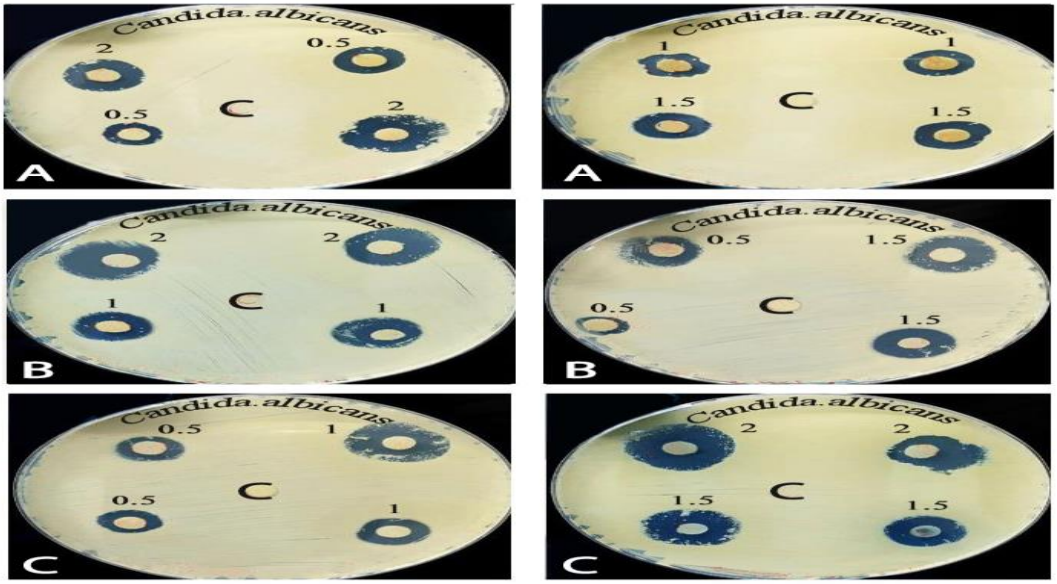

Figure 9. The effect of (A) CNPs, (B) CuNPs and (C) Cu/CNC on Candida albicans.

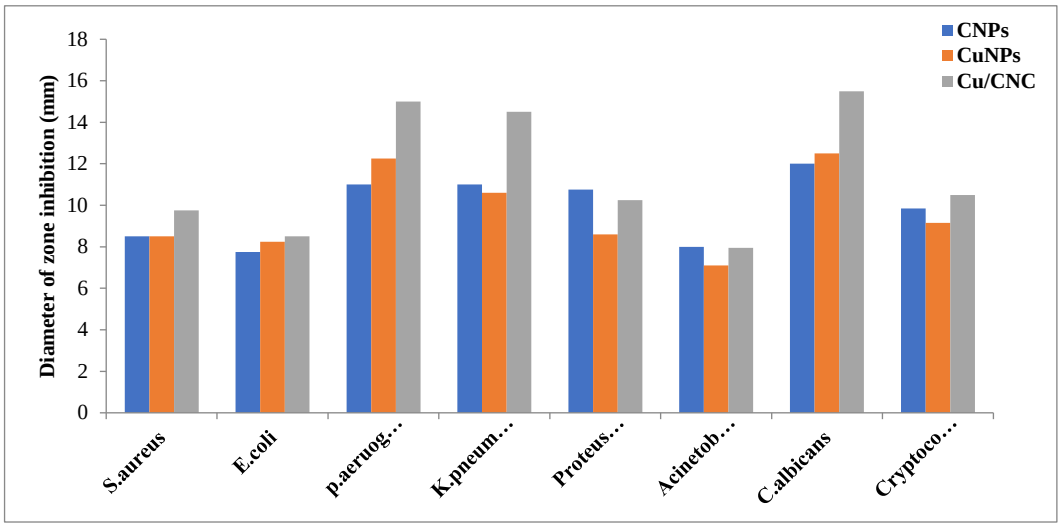

Figure 10. Antimicrobial activity of CNPs, CuNPs and Cu/CNC at concentrations 2 mg/ml.

Discussion

The XRD pattern of chitosan Fig. (1a) appeared at angles 2θ at 12.5°, 16.5°, 21.5°, 25.9°,32.5° and 38° corresponding to (300), (600), (110), (210), (103) and (101), this indicates formed crystal of chitosan nanoparticles as matched with [16]. The mean crystallite size of CNPs is 16.65nm, calculated by scheerer's equation (1).

$D = K\lambda / \beta\cos\theta$……(1)

D is the crystalline size of nanoparticles, K is 0.154, β is Full-Width Half at the Maximum (FWHM), and θ is Bragg angle. On the other hand, the XRD pattern of CuNPs Figure 1b was observed at angles 2θ = 36.40°, 43.5°, 50.5° and 74.5° corresponding to (101),(111),(200) and(220) that means high nanocrystalline of copper nanoparticles. The average crystallite size of CuNPs is 15.16nm, estimated by scheerer's equation and agreed with[17, 18]. Finally, the XRD pattern of Cu/CNC Fig.(1c) showed a broad peak at 25°, which indicated the chitosan amorphous structure because it interacted with copper nanoparticles. Moreover, the peak at 43° in agreement with the plane (111) attributed to the crystalline of copper nanoparticles, which refers to the CuNPs conjugated with CNPs successfully, as proved by [19].

The results of FTIR analysis for chitosan nanoparticles in Figure 2a showed that the characteristic peaks of CNPs were at 1543.05 cm-1 and 1627.92 cm-1, referring to the amino group and amide I, respectively. In comparison, 1519.91 cm-1 indicates the presence of an N-H deformation band of chitosan. Moreover, peaks of 1319.31 cm^{-1} and 1215.15 cm^{-1} were due to CH_2 stretching vibration. The bands at 1100-100 cm^{-1} are due to the saccharide structure of chitosan, as determined by [17, 20]. On the other hand, FTIR spectra for CuNPs are shown in Figure 2b; the peak at 3302.13 cm^{-1} indicates the stretching vibration of the O-H bond, while 1639.49 cm^{-1} refers to the stretching vibration of the Cu-O bond of copper oxide nanoparticles. Furthermore, the band at 594.08 cm-1, which is attributed to the bending vibration of the Cu-O bond and other bands, indicates the remains of materials used in the preparation of CuNPs, as obtained by [21]. FTIR analysis of

Cu/CNC is shown in the Figure 2c. The band at 1639.49 cm-1 was decreased to 1635.64 cm-1, while a new peak appeared at 2985.81 cm-1 attributed to C-H stretching of chitosan. Moreover, the bands 1651.07 cm-1, 1543.05 cm-1, 1523.76 cm-1, 1462.04 cm-1 and 1400.35 cm1 were deleted from FTIR spectra of Cu/CNC, and finally, the peak at 686.66 cm-1 refers to the interaction between copper and chitosan that agreed with results proved by [17, 22].

FE-SEM of CNPs are highly mono-dispersed spherical shape nanoparticles with a diameter average of 60-88 nm, as shown in Figure 3a; the CuNPs image appeared in the form of aggregated crystal cauliflower shape with bundles at the end it, with diameter average 14.14-20.12 nm, this suitable property for increasing surface to volume ratio of CuNPs for using as antimicrobial that lead to inhibiting growth of bacteria and fungi Figure 3b [23, 24]. Furthermore, Cu/CNC revealed aggregated, agglomerated and semi-spherical shapes with a diameter average of 36.34-48.27 nm Figure 3c. The EDS of CNPs shows peaks of C, O, P, N, Si, Na, Ca, and Mg. Nitrogen peak refers to the chitosan formed, as shown in Figure 4a, that agreed with [25]. Moreover, in Figure 4b, the EDS of CuNPs exhibit a high ratio of Cu and O, which means the copper is in oxidized form, as mentioned by [26]. The EDS of Cu/CNC, as shown in Figure 4c, shows peaks of C, O, N, P, and Cu. Nitrogen is attributed to chitosan binding to the CuNPs to form Cu/CNC, as proved by [27]. The increase in Zeta potential value refers to the increase in stability.

In Figure 6a, the ZP of CNPs was 10.7mV which indicates low stability of chitosan [28], but the ZP value of CuNPs was -44.4 mV, which means CuNPs had good stability because it oxidized [26], as seen in the Figure 6b. Moreover, the ZP of Cu/CNC was 15.8 mV, which is attributed to the increased stability of CNPs when binding with copper [29], as shown in Figure 6c.

The CNPs showed the highest effect against *S. aureus* and *P. aeruginosa*, as seen in Figures 7 and 8a. The variance in the results is attributed to the difference in the bacterial cell wall; gram-positive have a thick layer of peptidoglycan in their cell wall, which is made of a network having pores that allow foreign particles to enter the cell quickly. Whereas gram-negative have a thin layer of peptidoglycan in their cell wall and an outer membrane made up of lipoprotein, lipopolysaccharide, and phospholipid, which acts as a solid barrier to foreign particles due to it is bilayer structure [30,31,32]. CuNPs exhibit high antimicrobial activity against *C. albicans, P. aeruginosa, and S. aureus*, as seen in Figures 7, 8 and 9 b. The diversity of the results refers to differences in the bacterial cell wall, and CuNPs have a high surface-to-volume ratio so that they precipitate on the cell surface to form pores in the surface, then enter into the cell and release metal ions that cause damage to DNA and death [6,33,34]. Cu/CNC has higher antimicrobial activity than CNPs and CuNPs, as seen in Figure 10, which is attributed to the positively charged chitosan interaction with the negatively charged cell surface that enhances the entering of NPs into the cell and release metal ions that block intracellular components and cause cell death [35,36,37].

Conclusions

Cu/CNC was successfully prepared by a simple and low-cost method and then characterized. Cu/CNC appeared semi-spherical in shape with low stability. The antimicrobial activity of Cu/CNC was higher than that of CNPs and CuNPs. The antibacterial activity of Cu/CNC was higher against gram-negative than gram-positive strains. C. albicans looked more sensitive to the Cu/CNC among the fungal and bacterial strains in the present study.

Ethics approval: None required.

Conflict of interest: None declared.

Funding: No funding.

Acknowledgments: Our appreciation and gratitude to the Department of Applied Sciences at the University of Technology, Iraq.

References

1. Huynh, K. H., Pham, X. H., Kim, J., Lee, S. H., Chang, H., Rho, W. Y., & Jun, B. H. Synthesis, properties, and biological applications of metallic alloy nanoparticles. *International Journal of Molecular Sciences*, **2020**, *21*(14), 5174.
2. Venkatesh, N., Bhowmik, H., & Kuila, A. Metallic nanoparticle: a review. *Biomedical Journal of Scientific & Technical Research*, **2018**, *4*(2), 3765-3775.
3. Khandel, P., & Shahi, S. K. Microbes mediated synthesis of metal nanoparticles: current status and future prospects. *Int J Nanomater Biostruct*, **2016**, *6*(1), 1-24.
4. Arjunan, N., Singaravelu, C. M., Kulanthaivel, J., & Kandasamy, J. A. potential photocatalytic, antimicrobial and anticancer activity of chitosan-copper nanocomposite. *International journal of biological macromolecules*, **2017**, *104*, 1774-1782.
5. Tamilvanan, A., Balamurugan, K., Ponappa, K., & Kumar, B. M. Copper nanoparticles: synthetic strategies, properties and multifunctional application. *International Journal of Nanoscience*, **2014**, *13*(02), 1430001.
6. Din, M. I., Arshad, F., Hussain, Z., & Mukhtar, M. Green adeptness in the synthesis and stabilization of copper nanoparticles: catalytic, antibacterial, cytotoxicity, and antioxidant activities. *Nanoscale research letters*, **2017**,*12*(1), 1-15.
7. Covarrubias, C., Trepiana, D., & Corral, C. Synthesis of hybrid copper-chitosan nanoparticles with antibacterial activity against cariogenic Streptococcus mutans. *Dental materials journal*, **2018**,*37*(3), 379-384.
8. AL- Shamary, W. A. .; Alkhateb, B. A. A. H. .; Abdel, E. T. . Role Of Perlite Quantity And Intervals Of Irrigation On Potatoes (Solanum Tuberosum L.) Grown In Gypsiferous Soil. *Journal of Life Science and Applied Research*. **2020**, 1, 31-39.
9. Tyagi, A., Agarwal, S., Leekha, A., & Verma, A. K. Effect of mass and aspect heterogeneity of chitosan nanoparticles on bactericidal activity. *Int. J. Adv. Res*,**2014**, *2*(8), 357-367.
10. Resmi, R., Yoonus, J., & Beena, B. Anticancer and antibacterial activity of chitosan extracted from shrimp shell waste. *Materials Today: Proceedings*,**2021**, *41*, 570-576.

11. Fatma, S., Kalainila, P., Ravindran, E., & Renganathan, S. Green synthesis of copper nanoparticle from Passiflora foetida leaf extract and its antibacterial activity. *Asian Journal of Pharmaceutical and Clinical Research*, **2017**, 79-83.
12. A. Yaqub, N. Malkani, A. Shabbir, S. A. Ditta, F. Tanvir, S. Ali, M. Naz, S. A. R. Kazmi, and R. Ullah, "Novel Biosynthesis of Copper Nanoparticles Using Zingiber and Allium sp. with Synergic Effect of Doxycycline for Anticancer and Bactericidal Activity," Current Microbiology, **2020**, vol. 77, no. 9, pp. 2287–2299, Jun.
13. Agarwal, M., Agarwal, M. K., Shrivastav, N., Pandey, S., Das, R., & Gaur, P. Preparation of chitosan nanoparticles and their in-vitro characterization. *International Journal of Life-Sciences Scientific Research*, **2018**, *4*(2), 1713-1720.
14. Mohamed, E. A. Green synthesis of copper & copper oxide nanoparticles using the extract of seedless dates. *Heliyon*, **2020**, *6*(1), e03123.
15. Ibraheem M W, AL Mjbel A A, Abdulwahid A S, Mohammed Th. T. Characterization of the influence of diet on Japanese quail. *Revis Bionatura*. **2022**;7(4) 21. http://dx.doi.org/10.21931/RB/2022.07.04.21.
16. Thamilarasan, V., Sethuraman, V., Gopinath, K., Balalakshmi, C., Govindarajan, M., Mothana, R. A., ... & Benelli, G. Single step fabrication of chitosan nanocrystals using Penaeus semisulcatus: Potential as new insecticides, antimicrobials and plant growth promoters. *Journal of Cluster Science*, **2018**, *29*(2), 375-384.
17. Usman, M. S., El Zowalaty, M. E., Shameli, K., Zainuddin, N., Salama, M., & Ibrahim, N. A. Synthesis, characterization, and antimicrobial properties of copper nanoparticles. *International journal of nanomedicine*, **2013**, *8*, 4467.
18. AL-Jawad, S. M., Shakir, Z. S., & Ahmed, D. S. Antibacterial activity of Nickel-doped ZnO/MWCNTs hybrid prepared by sol–gel technique. *The European Physical Journal Applied Physics*, **2021**,*96*(2), 21201.
19. Ebrahimiasl, S., & Younesi, S. A. Shelf Life Extension of Package's Using Cupper/(Biopolymer nanocomposite) Produced by One-Step Process. *Journal of Food Biosciences and Technology*, **2018**, *8*(1), 47-58.
20. Huseen, R. H., Taha, A. A., Ali, I. Q., Abdulhusein, O. M., & Al-Jawad, S. M. Biological activity of gum Arabic-coated ferrous oxide nanoparticles. *Modern Physics Letters B*, **2021**, *35*(24), 2150411.
21. Raul, P. K., Senapati, S., Sahoo, A. K., Umlong, I. M., Devi, R. R., Thakur, A. J., & Veer, V. CuO nanorods: a potential and efficient adsorbent in water purification. *Rsc Advances*, **2014**, *4*(76), 40580-40587.
22. Alghamdi, K. S., Ahmed, N., Bakhotmah, D., & Mokhtar, M. Chitosan Decorated Copper Nanoparticles as Efficient Catalyst for One-Pot Multicomponent Synthesis of Novel Quinoline Derivatives: Sustainable Perspectives, **2018**.
23. Barbari, G. R., Dorkoosh, F. A., Amini, M., Sharifzadeh, M., Atyabi, F., Balalaie, S., ... & Tehrani, M. R. A novel nanoemulsion-based method to produce ultrasmall, water-dispersible nanoparticles from chitosan, surface modified with cell-penetrating peptide for oral delivery of proteins and peptides. *International journal of nanomedicine*, **2017**, *12*, 3471.
24. Ruman, U., Buskaran, K., Pastorin, G., Masarudin, M. J., Fakurazi, S., & Hussein, M. Z. Synthesis and characterization of chitosan-based nanodelivery systems to enhance the

anticancer effect of sorafenib drug in hepatocellular carcinoma and colorectal adenocarcinoma cells. *Nanomaterials*, **2021**, *11*(2), 497.

25. Rafigh, S. M., & Heydarinasab, A. Mesoporous chitosan–SiO2 nanoparticles: synthesis, characterization, and CO2 adsorption capacity. *ACS Sustainable Chemistry & Engineering*, **2017**, *5*(11), 10379-10386.
26. Al-Zharani, M., Qurtam, A. A., Daoush, W. M., Eisa, M. H., Aljarba, N. H., Alkahtani, S., & Nasr, F. A. Antitumor effect of copper nanoparticles on human breast and colon malignancies. *Environmental Science and Pollution Research*, **2021**, *28*(2), 1587-1595.
27. Hongfeng, Z., El-Kott, A., Ahmed, A. E., & Khames, A. Synthesis of chitosan-stabilized copper nanoparticles (CS-Cu NPs): Its catalytic activity for CN and CO cross-coupling reactions and treatment of bladder cancer. *Arabian Journal of Chemistry*, **2021**, *14*(10), 103259.
28. Gatta, A. K., Chandrashekhar, R., Udupa, N., Reddy, M. S., Mutalik, S., & Josyula, V. R. Strategic Design of Dicer Substrate siRNA to Mitigate the Resistance Mediated by ABCC1 in Doxorubicin-resistant Breast Cancer. *Indian Journal of Pharmaceutical Sciences*, **2020**, *82*(2), 329-340.
29. Bandara, S., Carnegie, C. A., Johnson, C., Akindoju, F., Williams, E., Swaby, J. M., ... & Carson, L. E. Synthesis and characterization of Zinc/Chitosan-Folic acid complex. *Heliyon*, **2018**,*4*(8), e00737.
30. Sarwar, A., Katas, H., & Zin, N. M. Antibacterial effects of chitosan–tripolyphosphate nanoparticles: impact of particle size molecular weight. *Journal of nanoparticle research*, **2014**, *16*(7), 1-14.
31. Al-Jawad, S. M., Taha, A. A., Redha, A. M., & Imran, N. J. Influence of nickel doping concentration on the characteristics of nanostructure CuS prepared by hydrothermal method for antibacterial activity. *Surface Review and Letters*, **2021**, *28*(01), 2050031.
32. Shakir, Z. S., AL-Jawad, S. M., & Ahmed, D. S. Influence of cobalt doping concentration on ZnO/MWCNTs hybrid prepared by sol-gel method for antibacterial activity. *Journal of Sol-Gel Science and Technology*, **2021**,*100*(1), 115-131.
33. Manikandan, A., & Sathiyabama, M. Green synthesis of copper-chitosan nanoparticles and study of its antibacterial activity. *Journal of Nanomedicine & Nanotechnology*, **2015**, *6*(1), 1.
34. Al-Jawad, S. M., Sabeeh, S. H., Taha, A. A., & Jassim, H. A. Synthesis and characterization of Fe–ZnO thin films for antimicrobial activity. *Surface review and letters*, **2019**, *26*(05), 1850197.
35. Syame, S. M., Mohamed, W. S., Mahmoud, R. K., & Omara, S. T. Synthesis of copper-chitosan nanocomposites and their applications in treatment of local pathogenic isolates bacteria. *Orient J Chem*, **2017**, *33*(6), 2959-2969.
36. AL-Jawad, S. M., Sabeeh, S. H., Taha, A. A., & Jassim, H. A. Studying structural, morphological and optical properties of nanocrystalline ZnO: Ag films prepared by sol–gel method for antimicrobial activity. *Journal of Sol-Gel Science and Technology*, **2018**, *87*(2), 362-371.
37. AL-Jawad, S. M., Taha, A. A., & Salim, M. M. Synthesis and characterization of pure and Fe doped TiO_2 thin films for antimicrobial activity. *Optik*, **2017**, *142*, 42-53.

Received: May 15, 2023/ Accepted: June 10, 2023 / Published: June 15, 2023
Citation: Ibadi G. K., Taha A. A., and Al-Jawad S. M. H.. Copper / Chitosan Nanocomposite Prepared by Chemical Method for Active Antimicrobial Activity. Revis Bionatura 2023;8 (3) 97. http://dx.doi.org/10.21931/RB/CSS/2023.08.03.97